X-661-71-297

PREPRINT

NASA TM X- 65668

LIMITS ON THE SMALL SCALE STRUCTURE OF THE DIFFUSE COSMIC X-RAYS

DANIEL A. SCHWARTZ
ELIHU A. BOLDT
STEPHEN S. HOLT
PETER J. SERLEMITSOS
R. D. BLEACH

JULY 1971

GSFC

GODDARD SPACE FLIGHT CENTER
GREENBELT, MARYLAND

LIMITS ON THE SMALL SCALE STRUCTURE OF THE DIFFUSE COSMIC X-RAYS

Daniel A. Schwartz*, Elihu A. Boldt, Stephen S. Holt, and Peter J. Serlemitsos
Goddard Space Flight Center
Greenbelt, Maryland 20771

and

Richard D. Bleach
University of Maryland
College Park, Maryland 20742

I. INTRODUCTION

In all popular theories, the diffuse cosmic X-rays contain a substantial contribution from sources at a redshift distance of order $z = 1$, thus measurement of their angular distribution provides data with cosmological relevance[1,2]. Wolfe and Burbidge[2] have constructed angular autocorrelation functions for X-rays arising directly or indirectly from the observed distribution of galaxies. Available data on the X-ray isotropy in the 10 to 40 keV range[3] had been obtained on an angular scale of 12°. To compare with that data, Wolfe and Burbidge had to integrate their autocorrelation functions to define an effective angular scale of fluctuations, and use beam convolution techniques[4] to extrapolate the measured upper limit X-ray fluctuations down to that angular scale. Here we compare the experimentally measured autocorrelation function with the calculations of Wolfe and Burbidge and confirm their conclusions that the X-ray isotropy is not consistent with the observed superclustering, and probably not with clustering, of galaxies. If the bulk of the diffuse cosmic X-rays arise from discrete sources, then the weakest lower limit to their number is obtained by ignoring possible clustering and yields a minimum of 5×10^5 objects assuming constant apparent luminosity or 4×10^6 objects assuming constant absolute luminosity.

*NAS-NRC Resident Research Associate

II. EXPERIMENTAL DETAILS

The X-ray detector consisted of a low-background multi-anode proportional chamber of 650 cm^2 effective area collimated 2° x 8° FWHM to a 3.2 cm^2 ster telescope factor. The counter contained one atmosphere of xenon-methane with a 25 μm mylar window. Events occuring in one and only one anode, and not vetoed by a simultaneous event in any immediately adjacent anode or in any of the anodes adjacent to the counter walls, entered the 128 channel analog to digital conversion. Our pulse height analyzer accepted events between 2 and 32 keV, giving a median energy of 6.3 keV for a diffuse X-ray count.

Aerobee flight 13.07 carried this detector to an altitude of 91 miles above White Sands Missile Range on September 21, 1970. We gathered spectral data from the Cygnus region and then searched for new sources between Cygnus and the known source Serpens XR-1. Using photographs of the star field, we verify that the rocket rolled the 2° aperture at about 0.51 degrees per second, along the galactic plane. During 44 sec., as the field of view moved from $\ell^{II} = 69°$ to $\ell^{II} = 46°$, we detected no discrete sources above a 3 σ limit of 0.02 photons $(cm^2 sec)^{-1}$ between 2 and 10 keV. We base the discussion in this letter upon the data obtained during this time.

Figure 1 presents our raw data vs. time sorted into bins of $\sim$ 2° width. The count rates shown represent mostly diffuse X-rays, but also contain some background due to electrons produced in the collimator and to high energy γ-rays which Compton scatter, depositing only a small fraction of their energy. The background spectrum is flat, with a small turn-up at a few keV. We have three independent estimates of the background flux: an upper limit of 10^{-3} $(cm^2keV)^{-1}$ obtained by viewing the earth in a previous rocket flight; an upper limit of 8×10^{-4} $(cm^2kev)^{-1}$ obtained by assuming all the measured counts above 25 keV were due to background; and similar numbers derived by comparing the measured count rates with rates predicted using the known detector response and the measured diffuse spectrum of $15.2E^{-1.7}$ above 8 keV[5] and $8.4\ E^{-1.35}$ below 8 keV[6]. From the last consideration, we consider the "noise" contribution as $\lesssim$ 25% for the data in Figure 1.

From the original results on an unresolved galactic component of X-ray emission[7], we would have expected 8 counts sec^{-1} due to galactic X-rays. Subtracting 20 seconds of data with the detector off the galactic plane* gives an estimate of only 4 $\pm$4 counts per second, a negligible contribution to the total diffuse count rate. Note, however, that Cooke and Pounds[9] report the resolution of the previously diffuse galactic component at $\ell^{II} \sim 300°$ into a few discrete X-ray sources which would lie above our present sensitivity. Thus we have no reason to expect such an extended galactic plane flux in the inter-arm region surveyed in this experiment.

III. LIMITS ON DISCRETE SOURCES

Let us assume that the diffuse X-rays arise as the integrated effect of discrete sources of constant apparent luminosity j (photons/sec), distributed uniformly randomly over the sky. Then in a set of bins containing

*The detector actually pointed at the Cygnus Loop during this time. To obviate our limit on galactic plane X-rays, this source would have to have a spectrum flatter than the diffuse component, whereas a previous measurement(8) shows this to have the softest known X-ray spectrum.

an average number of background counts C_b, we should observe a mean number of counts $\bar{N} = j\,\bar{n} + C_b$ and a variance in the number of counts $S^2 = j\,\bar{n}\,(j + 1) + C_b$.[10] From these relations we can calculate the average number of discrete sources in one bin on the sky: $\bar{n} = \frac{(\bar{N} - C_b)^2}{S^2 - \bar{N}}$. (If one considers that only a fraction f of the diffuse component is due to discrete sources then $\bar{n} = f^2 \frac{(\bar{N} - C_b)^2}{S^2 - N}$.) Lumping all the counts into $M = 11$ bins each 2° wide, we find $\bar{N} = 110$, $C_b = 27$, and the measured variance estimate $S^2 = \Sigma \frac{(N_i - \bar{N})^2}{10} = 62$. The data thus allows $S^2 - \bar{N} = 0$, $\bar{n} = \infty$. The variance in the estimate of S^2 is[11] $\text{var}\ S^2 = \frac{2}{M-1}\,(S^2)^2 = (28)^2$. Adding $3\sqrt{\text{var}\ S^2}$ to S^2, we estimate $(S^2 - N) \leq 36$, or $\bar{n} \geq 190$ to about 80% confidence. Since it takes 2600 of the 2° x 8° resolution elements to fill the sky, it would take at least 5×10^5 discrete sources to be consistent with the measured isotropy.

This compares with previous lower limits of 10^5 for the 10 to 40 keV range[3] and a limit (private communication from P. Sanford) of about 1.5×10^6 (to the same statistical significance)[12] obtained with an argon counter having a median energy of about 4 keV. Because the diffuse component has a complicated spectral shape, the predominant sources might differ as a function of energy and thus it is important to consider all the above limits as independent information concerning an appropriate range of energies.

Note that the limit obtained above applies only to sources of constant apparent luminosity. Sources of constant absolute luminosity distributed throughout a volume will add a term $\bar{n}$ var j to the expected variance, due to the dispersion in apparent emissivity proportional to $j^{-5/2}$.

We now expect $S^2 = j\,\bar{n}\,(j + 1) + \bar{n}\text{ var } j + C_b$. The total number of sources is still only proportional to the inverse square of the observed fluctuations, $\bar{n} = q\,(\bar{N} - C_b)^2/(S^2 - \bar{N})$ but is now multiplied by $q \equiv \langle j^2 \rangle / \langle j \rangle^2 \approx \frac{1}{3}\,\frac{r_o}{r_1}$, for a model of sources distributed within some maximum luminosity distance r_o, and where sources less distant than r_1 could be recognized individually. Our discrete source sensitivity stated previously gives us $r_1 \leq 4.3 \times 10^{26}$ cm, and taking $r_o = 10^{28}$ cm gives $q = 7.8$, or a lower limit of 4×10^6 sources of constant absolute luminosity in the sky. (If one asks how many of the discrete sources were recognized individually above a sensitivity F photons $cm^{-2}\ sec^{-1}$, then in surveying a fraction of the sky α one would expect on the average to detect $n = \frac{\alpha}{N^{1/2}} \left(\frac{4\pi\ I}{3\ F}\right)^{3/2}$ sources, where I is the average diffuse intensity, and N the total number of sources in the sky,[13,3] (cf. ref. 14, where $\delta I = 3\ F$). We observe no discrete sources, therefore to 98 percent confidence $n \leq 3$. We have $\alpha = 0.004$, giving us a lower limit of only 7000 sources using this technique, and we feel a previously published lower limit[12] of 10^9 sources should be corrected to a similarly small number.)

A much stronger lower limit is obtained if one considers the actual clustered distribution of galaxies instead of a random distribution. We compare with the calculations of Wolfe and Burbidge[2], who used the correlation technique developed by Chandrasekhar and Munch[15]. We divide our data into M = 220 bins of 0.205 seconds during the scan and construct the observed autocorrelation function $F(\theta) = f(\theta)/f(0)$,

$$f(\theta) = \frac{1}{M - k} \sum_{i=1}^{M-k} (N_i - \overline{N})(N_{i+k} - \overline{N})$$

where $\theta = 0.102\ k$ degrees, and $\overline{N}$ represents the average number of counts in one bin. We present the results in Figure 2, along with the previous theoretical calculation. Our data are consistent with random scatter about zero intrinsic correlation. The valid range of these measurements extend from the collimator resolution of 2° up to about 8°, where scatter increases due to the 23° limit of our scan. The data present a clear contradiction to supercluster and some cluster models for the origin of the diffuse X-rays. Independently, the data stand as a constraint to other theoretical calculations which might employ different cosmological models or connect the X-rays to galaxies in a manner different than the direct proportionality assumed by Wolfe and Burbidge.

References

1. Wolfe, A., Astrophys. J. (Letters) 159, L61 (1970).

2. Wolfe, A.M., and Burbidge, G.R., Nature 228, 1170 (1970).

3. Schwartz, D.A., Astrophys. J. 162, 439 (1970).

4. Conklin, E.K., and Bracewell, R.N., Nature 216, 777 (1967).

5. Schwartz, D.A., Hudson, H.S., and Peterson, L.E., Astrophys. J. 162, 431 (1970).

6. Boldt, E.A., Desai, U.D., Holt, S.S., and Serlemitsos, P.J., Nature 224, 677 (1969).

7. Cooke, B.A., Griffiths, R.E., and Pounds, K.A., Nature 224, 134 (1969).

8. Grader, R.J., Hill, R.W., and Stoering, J.P., Astrophys. J. (Letters), 161, L45 (1970).

9. Cooke, B.A., and Pounds, K.A., Nature 229, 144 (1971).

10. Schwartz, D.A., thesis, Univ. of California at San Diego (1969).

11. Guest, P.G., Numerical Methods of Curve Fitting (Cambridge; Cambridge University Press)(1961).

12. Fabian, A.C., and Sanford, P.W., Nature 231, 52 (1971).

13. Bunner, A.M., Coleman, P.C., Kraushaar, W.L., McCammon, D., Palmieri, T.M., Shilepsky, A., and Ulmer, M., Nature 223, 1222 (1969).

14. Silk, J., Space Sci. Rev. 11, 671 (1970).

15. Chandrasekhar, S., and Munch, G., Astrophys. J. 115, 103 (1952).

16. deVaucouleurs, G., Science 167, 1203 (1970).

FIGURE CAPTIONS

Figure 1. Total counts per 2.07° bin in galactic longitude. Fluctuations are consistent with counting statistics and allow no less than an average of 190 discrete sources to produce the total diffuse counting rate in each bin.

Figure 2. Autocorrelation functions. Solid lines: Theoretical calculations of Wolfe and Burbidge for superclusters (upper pair) or clusters (lower pair) of galaxies. The two lines in each pair are distinguished by the assumed total number of member galaxies. Triangles: Possible correlation modeled for our detector based on a 23° cut through contours of smoothed galaxy counts (to magnitude 19.4) presented by de Vaucouleurs[16]. Circles: Measured correlation, this experiment.

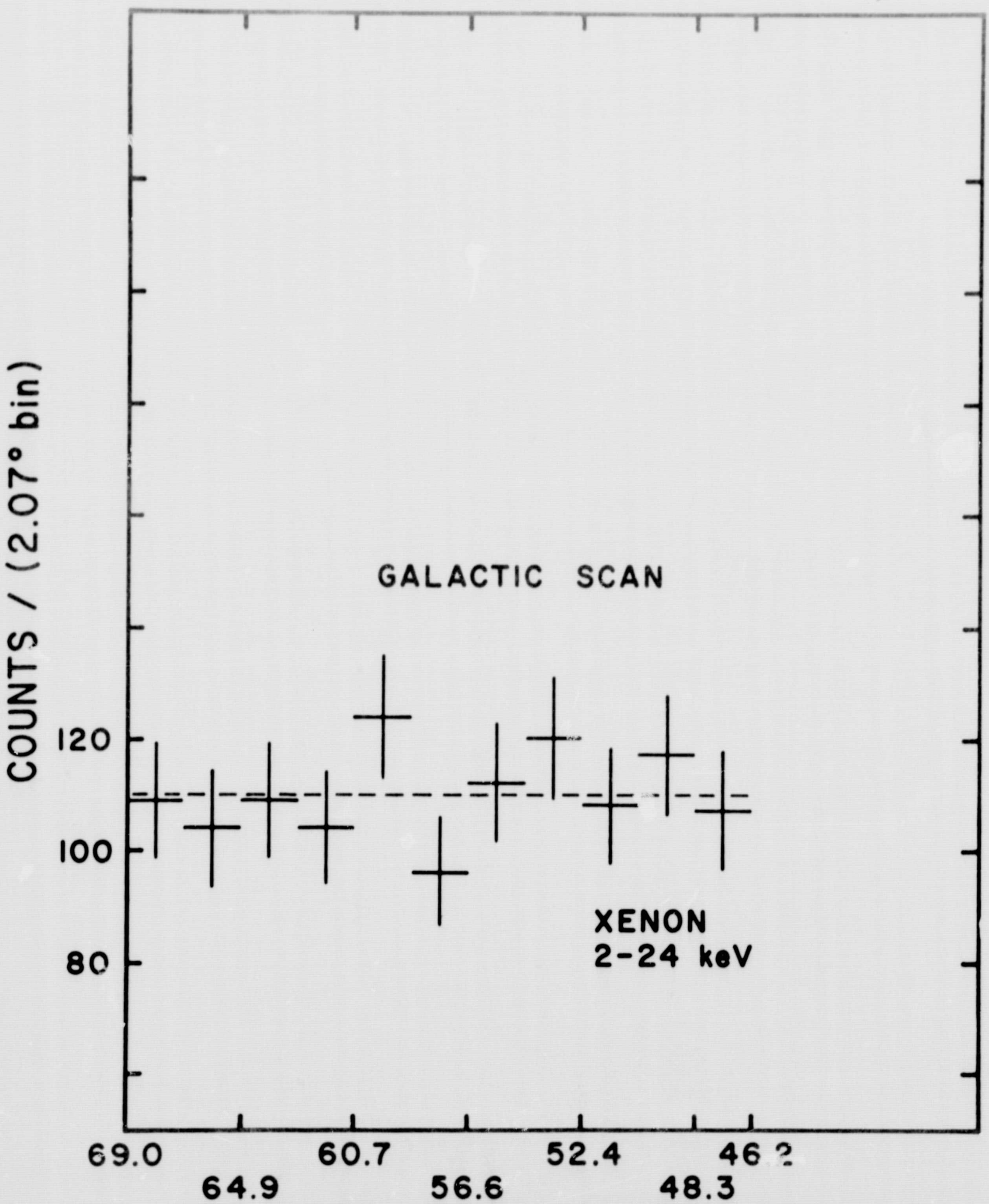
COUNTS / (2.07° bin)
GALACTIC SCAN
120
100
80
XENON
2-24 keV
69.0
64.9
60.7
56.6
52.4
48.3
46.2
GALACTIC LONGITUDE

FIGURE 1

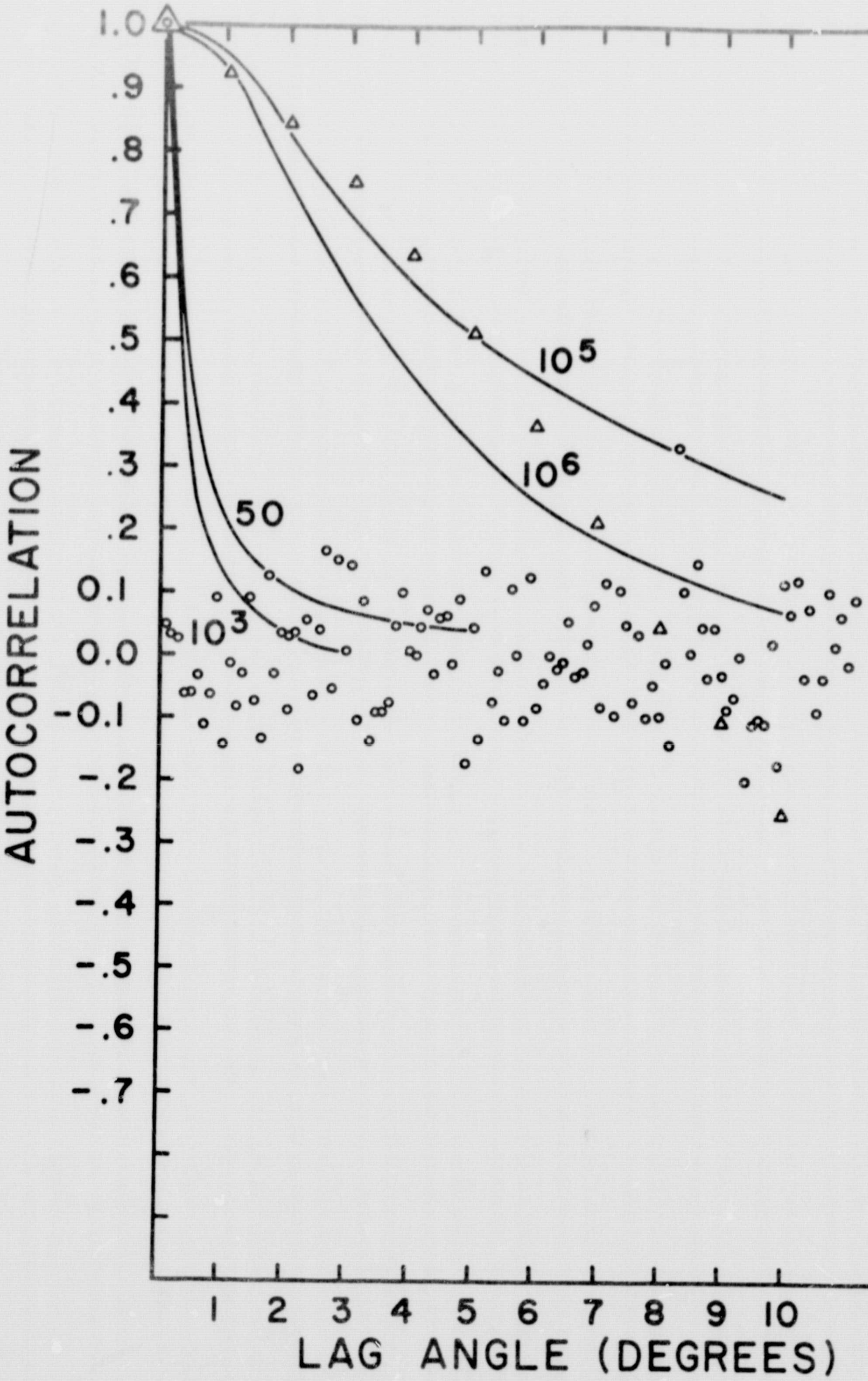

AUTOCORRELATION
1.0
.9
.8
.7
.6
.5
.4
.3
.2
0.1
0.0
-0.1
-.2
-.3
-.4
-.5
-.6
-.7
10^5
10^6
50
10^3
1
2
3
4
5
6
7
8
9
10
LAG ANGLE (DEGREES)

FIGURE 2